Targeted sortase A inhibition by novel peptidomimetic antivirulents against staphylococcal infections

AMERICAN SOCIETY FOR MICROBIOLOGY | Microbiology Spectrum

| Host-Microbial Interactions | Research Article

Targeted sortase A inhibition by novel peptidomimetic antivirulents against staphylococcal infections

Jordi C. J. Hintzen,[1,2] Shadi Rahimi,[3] Daniel Tietze,[1,2] Jian Zhang,[3] Priyanka Mehra,[1,2] Ivan Mijakovic,[3,4] Alesia A. Tietze[1,2]

AUTHOR AFFILIATIONS See affiliation list on p. 12.

ABSTRACT Antibiotic resistance is a critical public health issue, causing resistant bacterial strains to be increasingly difficult to control. Antivirulence therapies, which target bacterial virulence factors rather than kill bacteria, present a promising approach. Sortase enzymes, particularly SrtA, are crucial for gram-positive bacterial virulence by anchoring surface proteins essential for bacterial adhesion and biofilm formation to the bacterial outer cell wall. This study evaluates the selectivity of the peptidomimetic inhibitor BzLPRDSar toward various gram-positive bacteria. The BzLPRDSar significantly inhibited biofilm formation in multidrug-resistant *Staphylococcus aureus* and *Staphylococcus epidermidis*. Conversely, it showed variable and generally lower selectivity to gram-positive species such as *Enterococcus faecalis*, *Bacillus cereus*, and *Streptococcus agalactiae*. The selectivity toward *Staphylococcus* species is attributed to conserved structural elements in the SrtA enzyme, particularly the β7/β8 loop region with a key tryptophan, likely facilitating strong binding interactions with the inhibitor.

IMPORTANCE Antibiotic resistance is making it harder to treat bacterial infections, even with our strongest medicines. This study explores a new approach that does not aim to kill bacteria but instead disarms them by blocking the tools they use to cause disease. We focused on a bacterial enzyme called sortase A (SrtA), which helps harmful bacteria stick to surfaces and form protective layers called biofilms—structures that make infections very difficult to treat. We tested a specially designed molecule, BzLPRDSar, and found it could stop biofilm formation in drug-resistant strains of *Staphylococcus aureus* and *Staphylococcus epidermidis*. It was less effective against other bacteria, likely because of differences in the SrtA enzyme sequences. Our findings suggest that targeting virulence rather than killing bacteria may offer a safer and more sustainable way to treat infections, especially those caused by bacteria that no longer respond to antibiotics.

KEYWORDS antibiotic resistance, antivirulence, sortase A, inhibitors, peptidomimetics, *Staphylococcus*

Antibiotic resistance has become one of the most pressing public health challenges of the 21st century. The overuse and misuse of antibiotics in both human medicine and agriculture have accelerated the evolution of resistant bacterial strains. This resistance complicates the treatment of common infectious diseases and increases the risk of spreading resistant pathogens (1). For example, methicillin-resistant *Staphylococcus aureus* (MRSA) is responsible for severe infections that are difficult to treat and lead to high morbidity and mortality rates (2). Similarly, multidrug-resistant (MDR) *Enterococcus faecalis* and other gram-positive bacteria pose significant treatment challenges, often requiring the use of last resort antibiotics, further accelerating the development of resistance against these treatments (3). The development of new antibiotics has significantly slowed down over the past few decades due to high cost and the lengthy process of antibiotic research and development, coupled with lower financial incentives

Editor Gregory Wiedman, Seton Hall University, South Orange, New Jersey, USA

Address correspondence to Jordi C. J. Hintzen, Jordi.Hintzen@PennMedicine.upenn.edu, or Alesia A. Tietze, alesia.a.tietze@gu.se.

The authors declare no conflict of interest.

See the funding table on p. 12.

Received 30 July 2025
Accepted 14 January 2026
Published 3 March 2026

for pharmaceutical companies (4, 5). Moreover, the rapid emergence of resistance to new antibiotics further disincentivizes investment in antibiotic research. Given these critical issues, alternative strategies to combat bacterial infections are urgently needed. One promising approach is the development of antivirulence therapies. Unlike traditional antibiotics, which aim to kill bacteria, antivirulence therapies target the virulence factors bacteria use to establish infections and cause disease (6–8). By disarming the bacteria rather than killing them, these therapies exert less selective pressure for the development of resistance. This approach includes targeting specific bacterial processes such as toxin production, adhesion to host tissue, and biofilm formation (9, 10).

Among the virulence factors, sortase enzymes, found in all gram-positive bacteria, are among the most well studied. Sortases are a class of cysteine proteases responsible for anchoring surface proteins to the outer bacterial cell wall (11). Within the family of sortase enzymes found in different bacterial species, sortases A to F were described and differ in their primary sequence (12). Furthermore, sortase subtypes differ in their target proteins and have distinct biological roles. Within the target proteins, sortases recognize a short motif consisting of specific amino acids, where the enzyme can cleave and react with the substrate protein (13). These recognition motifs further define the subtype of a specific enzyme, which leads to the distinct roles of the subtypes within a bacterial species.

Arguably, the most important among this class of enzymes is sortase A (SrtA), which recognizes the LPxTG motif and anchors its target proteins to a Lipid II molecule (Fig. 1A) (13). The target proteins of SrtA are involved in bacterial adhesion to the host tissue and are defined by the umbrella term microbial surface components recognizing adhesive matrix molecules (MSCRAMMs). These MSCRAMMs adhere to the hosts' extracellular matrix proteins, such as fibrinogen and fibronectin, and are, therefore, crucial for the bacteria to invade their host (14). Additionally, SrtA is also required for proper adhesion of the bacteria amongst each other and plays an important role in the formation of pathogenic biofilms of many Gram-positive species (Fig. 1A) (15). These roles in bacterial physiology make SrtA a prime target for antivirulent therapy, as inhibition of this enzyme would lead to prevention of host tissue adherence as well as disruption of biofilm formation, leading to greatly reduced pathogenicity.

Diseases caused by gram-positive bacteria are often severe and highlight the critical need for new therapeutic strategies. For example, MRSA is notorious for its resistance to multiple antibiotics, making it a significant threat in both healthcare and community settings (2). Especially in infections like these, antivirulence could provide a crucial new treatment option. One disease that has been directly associated with SrtA is septic arthritis (16). Septic arthritis is a severe infection of the joints that can lead to permanent damage if not treated effectively (17). Here, SrtA inhibitors could serve as a first-line treatment option to combat septic arthritis. Biofilm formation is a common strategy employed by bacteria to protect themselves from the host immune system and antibiotics (18). Biofilms are complex communities of bacteria that adhere to surfaces and are embedded in a self-produced extracellular matrix. This matrix shields the bacteria from environmental stresses, making infections difficult to eradicate. Therefore, targeting biofilm formation, for example, by inhibiting SrtA, is a critical aspect of developing effective antivirulence therapies.

SrtA inhibitors have been an active research field, with numerous studies exploring their potential to reduce bacterial virulence and biofilm formation (19–22). Previously, we reported on the synthesis and evaluation of novel peptidomimetic substrate-derived SrtA inhibitors (Fig. 1A) (23). These compounds were active against expressed *S. aureus* SrtA with low micromolar IC_{50} values *in vitro*. Importantly, three compounds, BzLPRDSar, FLPRDA, and BzLPRDF, inhibited the growth of *S. aureus* and showed no killing activity on these bacteria. It was observed that the bacteria could still survive, but the plateau of the growth curve was significantly lower, suggesting a reduced ability to adhere to each other. BzLPRDSar, the compound with the largest effect on bacterial growth, was also

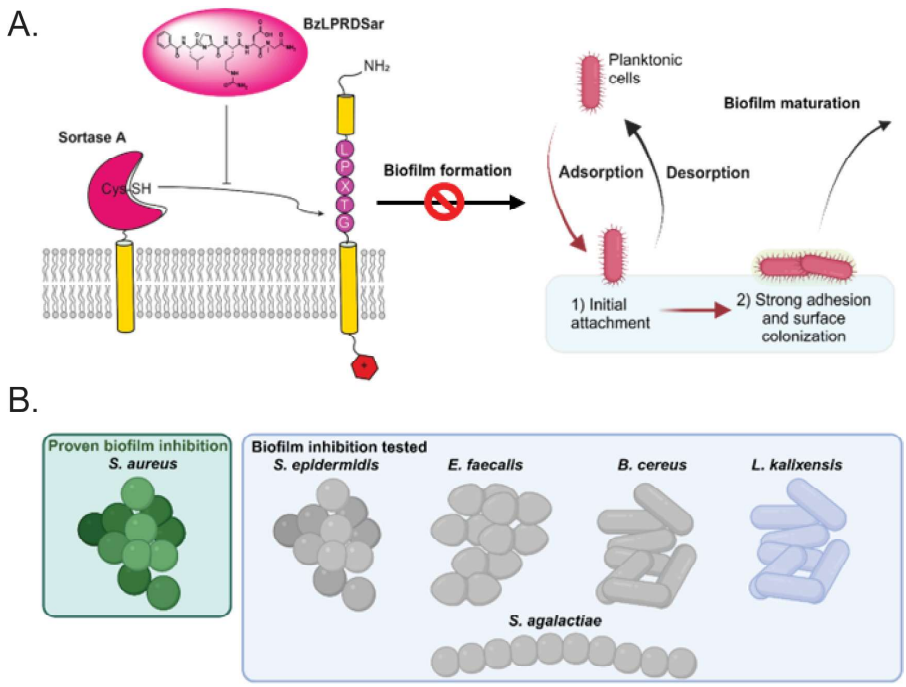

FIG 1 (A) Mechanism of action of peptidomimetic SrtA inhibitors to prevent biofilm formation (B) Overview of gram-positive strains that have been tested for biofilm inhibition by BzLPRDSar in this study.

tested for its ability to inhibit the biofilm formation of *S. aureus* and was able to eliminate 95% of the formed biofilms at 128 µg/mL.

Encouraged by the results when targeting *S. aureus*, we have now explored the potential of our lead peptidomimetic SrtA inhibitor, BzLPRDSar, against a variety of pathogenic and multidrug-resistant gram-positive bacteria (Fig. 1B). In our panel, we included a multidrug-resistant strain of *S. aureus* to verify the efficacy of our compounds in comparison to a wild-type *S. aureus* strain as was used earlier. Another multidrug-resistant bacterial species that was included is *E. faecalis*. *E. faecalis* is known to cause life-threatening infections such as endocarditis, sepsis, urinary tract infections, and meningitis. Particularly, *E. faecalis* forms persistently antibiotic-resistant biofilms, making it an excellent target for SrtA inhibition (24, 25). *Bacillus cereus* can cause foodborne illness due to its spore-forming nature; furthermore, biofilms formed by *B. cereus* pose a large challenge in the food production industry, as it grows readily on air-liquid interfaces and hard surfaces (26). Closely related to *B. cereus* is the species *B. anthracis*, which is well known as the anthrax bacteria and classified as a major pathogen within the *Bacillus* genus (27). The next species we included in the panel, *Lactobacillus kalixensis*, is known to form biofilms in the vaginal and gut microbiota, where it can become pathogenic (28). Importantly, *L. kalixensis*, as with other lactobacilli, grows under anaerobic conditions. As a representative of the *Streptococcus* genus, *Streptococcus agalactiae* was included, which is the most common human pathogen of the streptococci. It can cause severe invasive infections in the elderly, newborns, and immunocompromised patients (29). *S. agalactiae* is also a common bovine pathogen as it is the main cause of bovine mastitis, making treatment of this bacterium very relevant for veterinary medicine as well (30). Finally, *Staphylococcus epidermidis*, a species found in the normal skin and sometimes the mucosal microbiota, was included. In some cases, *S. epidermidis* can cause dangerous infections and is notoriously hard to treat (31).

Comparing these bacterial species gives us a wide variety of distinctly different pathogenic gram-positive bacteria, ranging from several major families, providing insight into the potential of our peptidomimetic SrtA inhibitors as a pan-SrtA inhibitor, which could be applied to treat widely different infections. Furthermore, these pathogens are

involved in many different disease phenotypes in humans but also stretch to veterinary medicine and the food industry, conceivably increasing the scope of the potential of these inhibitors. Therefore, we have investigated the effect of our previously discovered lead compound, BzLPRDSar, on the growth and biofilm formation of these bacteria (23).

RESULTS AND DISCUSSION

From our initial panel, several compounds were able to affect the growth of *S. aureus* bacteria; however, BzLPRDSar stood out among these as the compound with the largest effect on the growth profile of *S. aureus* and additionally was able to efficiently disrupt biofilm formation of this species at concentrations as low as 32 µg/mL, making it the compound of choice for testing toward other bacterial species (23). It was synthesized and purified according to previously reported procedures and subsequently used in the bacterial assays (Fig. S1). For the growth profiling assays, the different bacterial species were grown in Tryptic Soy Broth (TSB), transferred to a 96-well plate, and subsequently incubated with varying concentrations of BzLPRDSar, at 2, 8, 32, and 128 µg/mL. To allow the multidrug-resistant species to grow optimally, *S. aureus*, *E. faecalis*, and *K. pneumoniae* were grown and incubated in Mueller Hinton Broth (MHB), while *L. kalixensis* was grown and incubated under anaerobic conditions in TSB in an atmosphere consisting of 5% CO_2 and 6% O_2. As a negative control, the gram-negative bacterial species *Klebsiella pneumoniae* was included in the panel, which lacks SrtA altogether and is, therefore, not expected to be affected by our peptidomimetic inhibitor. Overall, the same trend as reported previously was observed, where the bacteria grew in the first 6–12 h undisturbed (Fig. 2) and only after reaching their respective plateaus, a difference in their growth profile could be observed. Interestingly, different bacterial species showed vastly different growth profiles, but consistently, the plateau was reached after 48 h of incubation and was used as a measure to define their growth decrease when treated with BzLPRDSar. Comparatively, the MDR strain of *S. aureus* was affected to a lesser extent than the previously used wild-type strain (Fig. 2A) (23). Whereas BzLPDRSar displayed a 36% decrease in growth at 128 µg/mL for the wild-type strain, only a 10% decrease could be observed for the MDR strain, suggesting its more persistent nature (Table 1). However, other bacterial species were efficiently inhibited in their growth at this concentration, with multidrug-resistant *E. faecalis*, *B. cereus*, and *S. epidermidis* showing moderate growth inhibition at around 20% (Table 1; Fig. 2B through D). *S. agalactiae* proved to be the species least efficiently affected among the tested gram-positive species, showing only an 8.9% decrease at 128 µg/mL (Table 1; Fig. 2E). Fortunately, the gram-negative *K. pneumoniae* was not significantly inhibited, showing a negligible decrease in growth at even the highest inhibitor concentration present, further confirming that the presence of SrtA in gram-positive species is needed for efficient growth inhibition (Table 1; Fig. S2). Finally, *L. kalixensis* was the species that was most affected by our peptidomimetic inhibitor, showing a 42% decrease in growth at 128 µg/mL, outperforming the originally tested *S. aureus* strain (Table 1; Fig. 2F). This finding could potentially be due to the difference in growth conditions used for the anaerobic *L. kalixensis* strain. Furthermore, it is possible that *L. kalixensis* is less efficient in degradation and clearance of the drug during the growth profiling experiments in comparison to the other bacterial species tested. Taken together, these results show that gram-positive bacteria are indeed specifically targeted by BzLPRDSar at varying degrees, differing from species to species. However, as all these species grow pathogenic biofilms that can cause major threats in health, the ability of BzLPRDSar to disrupt these biofilms was assayed for all gram-positive species. Statistical significance between different concentration groups at each time point was assessed using the non-parametric Kruskal–Wallis test. This test compares median ranks among multiple groups without assuming normal data distribution. The analysis revealed significant differences (P = 0.01–0.04), indicating that bacterial growth was affected by the tested concentrations.

Bacterial biofilms were generated as previously described by incubating varying concentrations of BzLPRDSar in Brain Heart Infusion Broth on coagulase-coated 96-well

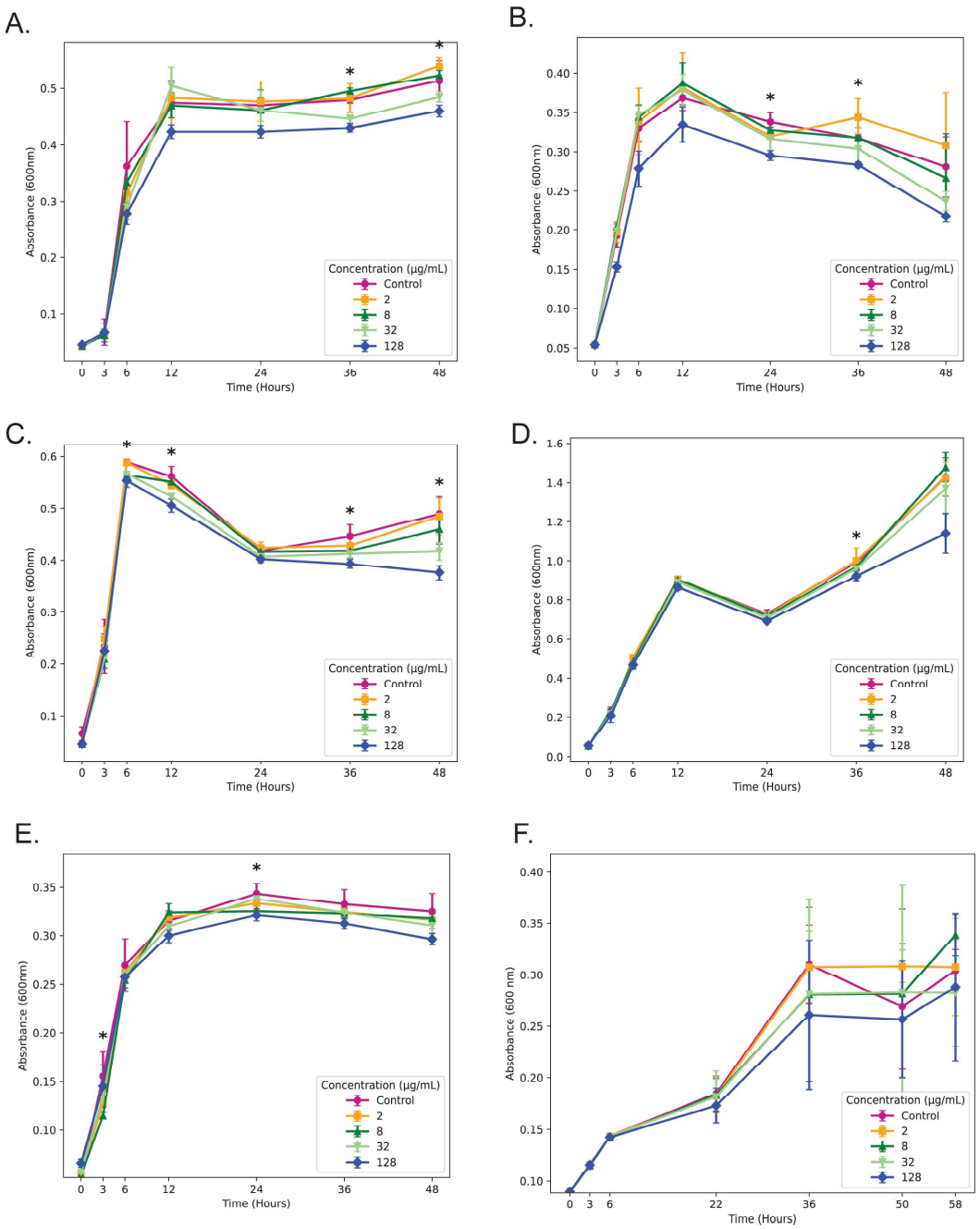

FIG 2 Growth profiling curves of bacteria incubated in the presence of varying concentrations of BzLPRDSar. The absorbance was measured at 600 nm as a measure of OD for (A) *S. aureus* multidrug resistant (MDR); (B) *S. epidermidis*; (C) *E. faecalis* MDR; (D) *B. cereus*; (E) *S. agalactiae*; and (F) *L. kalixensis*. All samples were measured in triplicate, and error bars are reported as standard error (±SE). Kruskal–Wallis statistical analysis was performed at each timepoint to assess differences among concentrations; stars (*) indicate timepoints with statistically significant differences ($P < 0.05$).

plates (23). After an overnight incubation with the peptidomimetic inhibitors, bacterial biofilms were stained with crystal violet (CV) and solubilized in 90% ethanol to quantify the remaining amount of biofilm by measuring the absorbance at 595 nm (Fig. S3). As was reported before, the formation of *S. aureus* biofilms at concentrations of 32 and 128 µg/mL of BzLPRDSar was efficiently inhibited, in line with previously reported values, with 34% and 26%, respectively, of remaining biofilm (Fig. 3; Table 2). In line with growth inhibition, the MDR *S. aureus* strain used in these experiments

TABLE 1 Growth profiling overview

Species	Decrease in growth 32 µg/mL, %	Decrease in growth 128 µg/mL, %
Staphylococcus aureus MDR	6 ± 1	10 ± 2
Staphylococcus epidermidis	16 ± 4	22 ± 1
Enterococcus faecalis MDR	6 ± 5	23 ± 3
Bacillus cereus	4 ± 7	20 ± 7
Streptococcus agalactiae	5 ± 2	9 ± 1
Lactobacillus kalixensis	17 ± 4	42 ± 3
Klebsiella pneumoniae MDR	2 ± 1	2 ± 1

proved to be slightly more resistant to treatment with the peptidomimetic than its wild-type counterpart. Surprisingly, an efficient disruption of biofilm formation was also observed for *S. epidermidis* at these inhibitor concentrations, with 48% and 36% of biofilm remaining, respectively (Table 2; Fig. 3). Seemingly, BzLPRDSar only had a moderate effect on the growth profile of *S. epidermidis* but was able to disrupt the formation of biofilms quite efficiently in this species. Among the other included bacterial species, biofilm inhibition proved to be less efficient than for the two *Staphylococcus* species tested, with around 60%–70% of biofilm remaining for *E. faecalis*, *B. cereus*, and *L. kalixensis* at 128 µg/mL and even 90% for *S. agalactiae* at this concentration (Table 2; Fig. 3). While *L. kalixensis* showed promising results when examining its growth profile, the biofilms formed by this bacterial species proved to be resistant toward treatment with our peptidomimetic inhibitor (Table 2; Fig. 3). To assess whether the observed differences in biofilm formation across the tested concentrations of BzLPRDSar were statistically significant, absorbance values from triplicate measurements were analyzed by one-way ANOVA for each bacterial species. When overall differences were detected, Tukey's HSD post hoc test was used to determine which concentration pairs differed significantly. Significant differences ($P < 0.05$) are indicated by dotted brackets in the figure. All in all, it can be observed that a certain degree of selectivity is displayed in the biofilm inhibition experiments, where BzLPRDSar was efficient in disrupting biofilms of the genus *Staphylococcus* but did not show a considerable effect on biofilms of other species, providing an opportunity to selectively use these compounds to target *Staphylococci* infections.

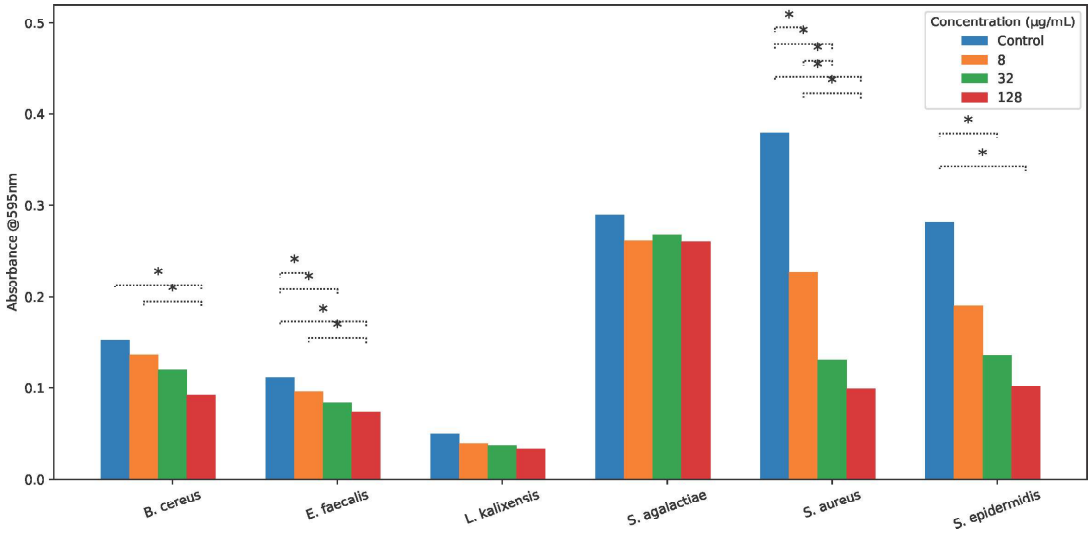

FIG 3 Absorbance measurements of bacterial biofilms stained with crystal violet, which were incubated with varying concentrations of BzLPRDSar. Absorbance was measured at 595 nm; samples were taken in triplicate, and error bars were reported as standard error (±SE). Statistical significance was assessed using one-way ANOVA followed by Tukey's HSD post hoc test for multiple comparisons within each bacterial strain. Significant differences (*$P < 0.05$) are indicated by dotted brackets.

TABLE 2 Biofilm inhibition overview (MBIC: Minimal biofilm inhibition concentration) (32)

Species	Biofilm remaining 32 µg/mL, %	Biofilm remaining 128 µg/mL, %	MBIC, µg/mL
Staphylococcus aureus MDR	34	26	32
Staphylococcus epidermidis	48	36	32
Enterococcus faecalis MDR	74	66	>128
Bacillus cereus	79	61	>128
Streptococcus agalactiae	93	90	>128
Lactobacillus kalixensis	69	65	>128

To elucidate the molecular basis for the observed specificity of BzLPRDSar toward *Staphylococcus* species, we conducted a detailed sequence alignment of the SrtA enzymes from the various bacterial species included in our study using Jalview and ClustalΩ (19, 33, 34). Strikingly, several key structural elements are conserved among the aligned *Staphylococcus* species but vary greatly among the other evaluated species. The β2/H1 loop region, which is known to be involved in substrate binding, consists of the neutrally charged PATP sequence in *S. aureus*, *S. epidermidis*, *Staphylococcus capitis*, *Staphylococcus haemolyticus*, and *Staphylococcus lugdunensis*, while in many other species, negatively or positively charged amino acids appear (35, 36). Furthermore, the β6/β7, also involved in substrate binding, shows some sequence similarity between the staphylococci, while it varies to a bigger extent among the other species (37, 38). Perhaps most striking is the β7/β8 loop region, which is extended in a similar manner only in the staphylococcal SrtA proteins, whereas this region is significantly shorter in other species. It was shown earlier that the β7/β8 loop region has an influence on the binding of peptidomimetic inhibitors and is therefore suspected to play a role in the selectivity of BzLPRDSar as well (38).

The alignment also revealed a notable difference in the amino acid sequences in the β7/β8 loop, particularly highlighting a single tryptophan residue at position 194 for *S. aureus* (W194) or position 191 for *S. epidermidis* (W191) in the elongated β7/β8 loop (Fig. 4A). The tryptophan residue present here in *Staphylococcus* species is absent in the SrtA sequences of the other gram-positive bacteria tested in our panel, such as *E. faecalis*, *B. cereus*, and *S. agalactiae*. Our computational analysis conducted earlier suggested that the aromatic side chain of the tryptophan residue at this position forms some key interactions with the Sar residue of the BzLPRDSar molecule (Fig. 4B) (23). This interaction likely stabilizes the binding of the inhibitor to the active site of the enzyme, enhancing its inhibitory potency. In the absence of this tryptophan residue in other bacterial species, such stabilizing interactions are not possible, which could explain the reduced efficacy of BzLPRDSar against these non-staphylococcal SrtA enzymes (Fig. 4A and B). Also, the physicochemical properties and thus the overall shape of the active site varies slightly among the different species, as can be concluded from the sequence alignment and Fig. 4C and D. As stated earlier, the flexible β7/β8 loop has a strong influence on the shape and properties of the binding site and seems to play a key role in inhibitor binding similarly as it is a major player to alter substrate specificity among sortase enzymes (39). An exception is *L. kalixensis*, which showed promising results in growth inhibition assays but only moderate biofilm inhibition. While *L. kalixensis* does possess a tryptophan residue in the active site, it is in a slightly different location. Moreover, the surrounding defining loop regions (Fig. 4A) are vastly different from SrtA from *S. aureus* and *S. epidermidis*, providing a reasonable explanation for the difference in effectivity of BzLPRDSar.

The highly similar loop regions and the unique presence of this tryptophan in *Staphylococcus* species provide a structural rationale for the selective inhibition observed in our growth and biofilm assays. The strong interaction between BzLPRDSar and the W194 residue effectively aids the disruption of the SrtA function in *S. aureus* and *S. epidermidis*, leading to the observed significant reductions in bacterial growth and biofilm formation. In contrast, the lack of this residue in other species, in combination

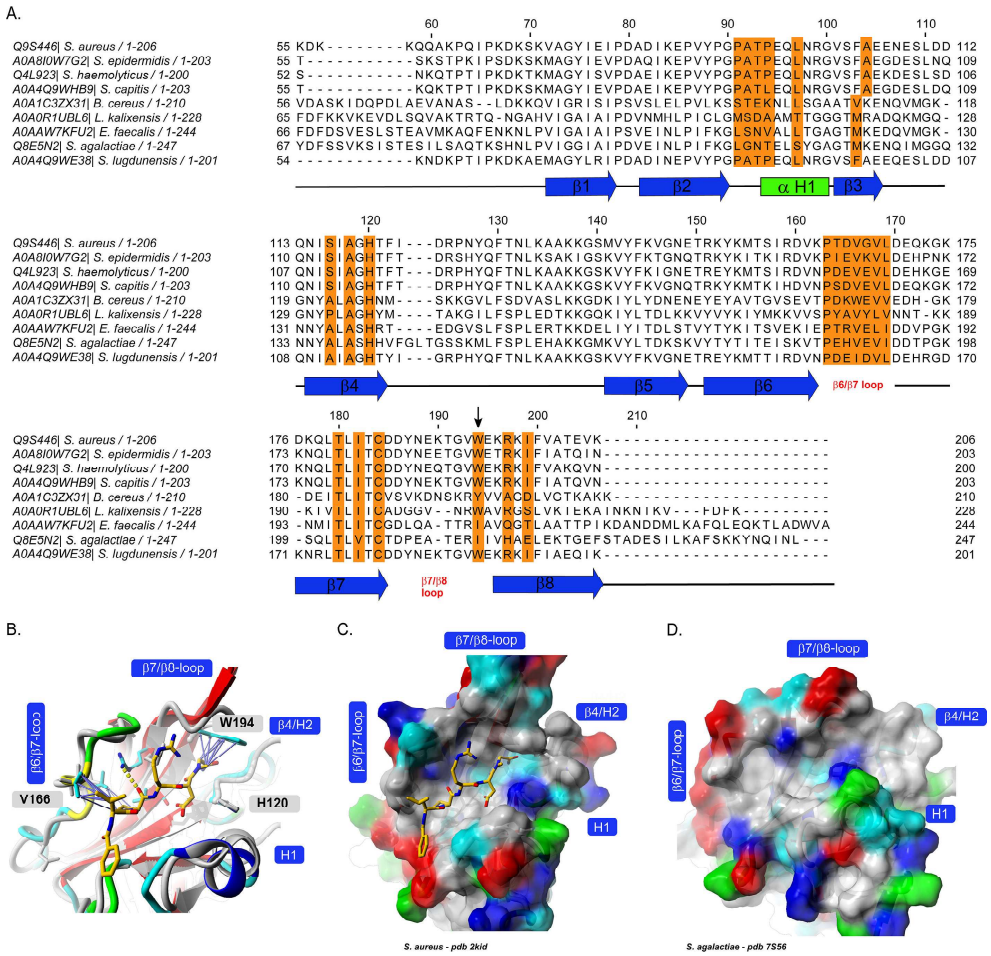

FIG 4 (A) Sequence alignment of the SrtA enzymes from the studied bacterial species. Highlighted in orange are residues in and around the substrate binding site, while secondary structure elements are indicated with lines and arrows underneath the sequence alignment. W194, as a potential key residue for inhibitor binding affinity, is indicated with an arrow. (B) Structural alignment of *S. agalactiae* (gray) and *S. aureus* SrtA bound to BzLPRDSar (colored) highlighting some key Van-der-Waals interaction (purple arrows) to W194 and V166 (protein structures shown in ribbon style, ligand and some interacting protein side chains shown in stick representation, color scheme: ligand carbon, orange; protein side chain carbon, cyan; nitrogen, blue; oxygen, red). (C and D) Surface representation of *S. aureus* SrtA with bound inhibitor (same coloring scheme as in B) and *S. agalactiae* SrtA (surface colored according to the physicochemical properties of the amino acids, color scheme: polar, cyan; green; unpolar, gray; red, acidic; blue, basic). Structure views created with Yasara (40, 41).

with critical differences in the loop regions, results in a less effective binding of the inhibitor, thereby reducing its impact on their growth and biofilm development.

Finally, we performed scanning electron microscopy (SEM) imaging for *S. aureus* and *S. epidermidis* biofilms to observe potential structural changes in the bacterial cellular membrane and the interbacterial association within the biofilm (42). Earlier, confocal microscopy could confirm some differences in overall colony formation and morphology of *S. aureus* treated with peptidomimetic inhibitors (23). Staphylococcus biofilms were grown directly on SEM glass cover slides and incubated with BzLPRDSar at a concentration of 128 µg/mL, a concentration that could eliminate a major part of the biofilms when grown on a coagulase substrate (Table 2). After 18 h of incubation with the peptidomimetic compound, the bacteria were fixed using glutaraldehyde and subsequently incubated with increasing concentrations of ethanol, ranging from 40% to 100%. After the final ethanol step, the samples were dried and coated with a 5 nm gold layer and directly measured.

SEM measurements revealed notable differences in the structural integrity and interbacterial associations within the biofilms of *S. aureus* and particularly of *S. epidermidis* when treated with BzLPRDSar. For both species, the untreated biofilms displayed a typical multi-layered structure with tightly associated bacterial cells (Fig. 5; Fig. S4) (43). The cellular membranes of the treated *S. aureus* appeared slightly smoother compared to the untreated control, suggesting potential membrane remodeling or stress responses induced by the inhibitor (Fig. 5A). For *S. epidermidis*, the treated biofilm structure was markedly disrupted. The cells appeared more globular and less interconnected, indicating a significant reduction in interbacterial adhesion and biofilm integrity (Fig. 5B). These structural changes confirm the biofilm inhibition data, highlighting the efficacy of BzLPRDSar in disrupting biofilm formation in *Staphylococcus* species. Cell circularity was quantified from SEM images (Fig. S5). Treated cells exhibited significantly higher circularity compared with control cells, indicating that interconnectivity between cells was reduced due to inhibition of SrtA. Statistical significance was assessed using the two-tailed Mann–Whitney *U* test. Data are presented as mean ± SD. A total of $n = 50$ cells per condition were analyzed.

In this study, we evaluated the selectivity of our lead peptidomimetic SrtA inhibitor, BzLPRDSar (23), in inhibiting the growth and biofilm formation of a variety of pathogenic gram-positive bacterial species. Our findings indicate that BzLPRDSar is highly effective in inhibiting both the growth and biofilm formation of *S. aureus*, including the evaluated MDR strain, as well as *S. epidermidis*. BzLPRDSar disrupted biofilm formation to a notable extent, with only 26% and 36% of biofilm remaining for *S. aureus* and *S. epidermidis*, respectively, at the highest concentration of 128 µg/mL tested. Importantly, compared to the previously used *S. aureus* strain (23), BzLPRDSar was still effective toward the MDR strain used in this study, suggesting a robust strain-to-strain effectiveness within the same species. The selective inhibition can be attributed to the unique structural features of the peptidomimetic compound. Sequence alignment revealed that staphylococcal SrtA enzymes possess a tryptophan residue near the active site, which appears to be specifically targeted by the C-terminal sarcosine (Sar) residue of BzLPRDSar. This molecular interaction likely enhances the binding affinity and inhibitory potency of BzLPRDSar against staphylococcal SrtA, explaining its preferential activity. The identification of the W194 residue (or W191 in *S. epidermidis*) highlights our rational design strategy for inhibitor design in developing targeted antimicrobial therapies. This approach not only enhances the selectivity of the inhibitors against specific pathogens but also can minimize off-target effects. These findings provide a compelling explanation for the selective activity of BzLPRDSar and pave the way for further optimization and development of targeted SrtA inhibitors. Additionally, SEM analysis of *S. epidermidis* treated with BzLPRDSar revealed that the association between bacteria was significantly disrupted. This morphological evidence supports the hypothesis that BzLPRDSar impairs the adhesion processes mediated by MSCRAMMs, which are anchored to the cell wall by SrtA. By inhibiting SrtA, BzLPRDSar prevents the proper attachment of these surface proteins, leading to a failure in biofilm formation and inter-bacterial cohesion.

All in all, our results demonstrated that BzLPRDSar is selective toward *Staphylococcus* species, which could provide an opportunity for developing targeted therapies that can effectively combat staphylococcal infections without broadly disrupting the microbiome. This selective action could prevent the common side effects associated with broad-spectrum antibiotics, such as dysbiosis and disruption of beneficial microbial communities. However, *in vivo* studies are essential to validate the therapeutic potential of these compounds in animal models of staphylococcal infections. Encouragingly, a related peptidomimetic SrtA inhibitor, LPRDA, was recently shown to be efficient *in vivo* in the treatment of peritoneal infections of *S. aureus* in mice, highlighting the potential of this class of compounds even further (44). The development of these targeted antivirulence therapies has the potential to revolutionize the treatment of bacterial infections, offering a new strategy to combat antimicrobial resistance.

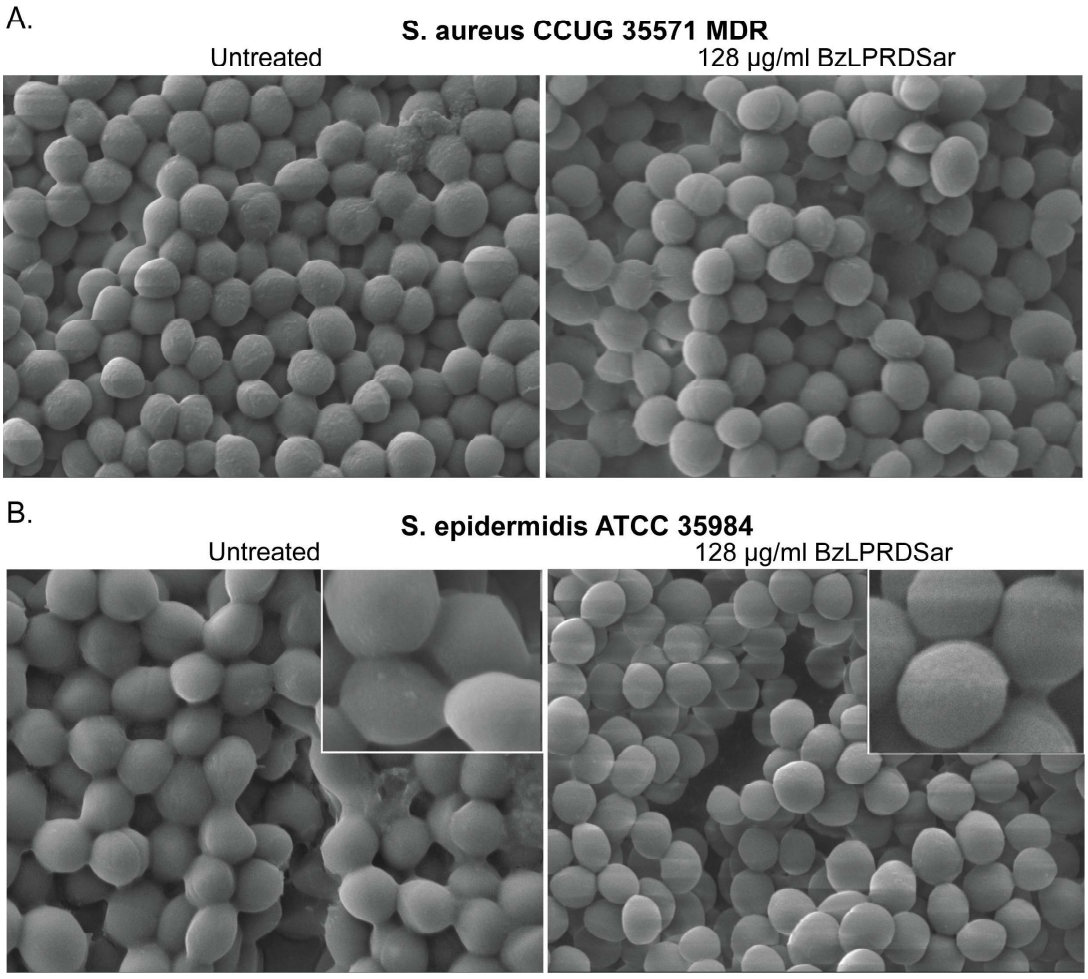

FIG 5 Scanning electron microscopy (SEM) images illustrating structural changes in biofilms of *S. aureus* and *S. epidermidis* incubated with 128 µg/mL of BzLPRDSar for 18 h. Magnification 15,000×, with insets at 50,000×. (A) SEM images of *S. aureus* biofilms, untreated control (left), and treated biofilm (right). (B) SEM images of *S. epidermidis* biofilms, untreated control (left), and treated biofilm (right).

MATERIALS AND METHODS

Peptide synthesis and purification

Peptidomimetic inhibitor BzLPRDSar was synthesized according to previously reported procedures (23). Briefly, the peptide was chain assembled using Rink amide resin manually. Amino acid couplings were carried out with the molar ratio of 4:4:8 (Fmoc-protected amino acid:HATU:diisopropylethylamine) at room temperature for 60 min, and deprotection was achieved in 20% piperidine in N,N-dimethylformamide (DMF) for 30 min at room temperature. N-terminal benzoylation was achieved with benzoyl chloride (10 eq.) and triethylamine (10 eq.) in DMF for 2 h at room temperature. The peptide proceeded to standard cleavage from resin using a mixture of trifluoroacetic acid (TFA, 95%), H_2O (2.5%), and triisopropylsilane (2.5%) for 3 h at room temperature. TFA was removed using N_2, and the resultant residue was suspended in ice-cold diethyl ether. The mixture was then centrifuged (5 min, 4,600 RPM), after which the supernatant was decanted into the waste. The remaining solid was washed twice with ice-cold diethyl ether and subjected to purification. For the purification and characterization of peptides, two eluent systems were used. Mobile phase A was 0.1% TFA in MQ-H_2O, mobile phase B was 0.1% TFA in acetonitrile (ACN). The crude peptide was dissolved in a mixture of ACN in H_2O and purified by semi-preparative high-performance liquid chromatography (HPLC) using a Waters 600 system equipped with a C18 column (Multokrom 100-5 C18,

5 µm particle size, 100 Å pore size, 250 × 20 mm) and a gradient of mobile phase A and mobile phase B from 20% B to 60% B over 45 min at 8 mL/min. Detection of chromatographic peaks was analyzed at 214 and 254 nm. Analytical RP-HPLC was carried out on a Waters XC e2695 system employing a Waters PDA 2998 diode array detector equipped with a ISAspher 100-3 C18 (C18, 3.0 µm particle size, 100 Å pore size, 50 × 4.6 mm) at a flow rate of 2 mL/min using a gradient of mobile phase A and mobile phase B from 20% B to 60% B over 10 min. The molecular weight of the purified peptide was confirmed by ESI mass on a Waters Synapt G2-Si ESI mass spectrometer equipped with a Waters Acquity UPLC system using a Xela C18 column (C18, 1.7 µm particle size, 80 Å pore size, 50 × 3.0 mm).

Growth profiling assays

For the growth profiling experiments, *S. aureus* strain CCUG 35,571, *E. faecalis* strain CCUG 34,289, and *K. pneumoniae* strain CCUG 37,387 were cultured overnight in sterile MHB medium, while *B. cereus* strain UW85, *S. agalactiae* strain CCUG 4208T, and *S. epidermidis* strain ATCC 35,984 were cultured overnight in sterile TSB medium. *L. kalixensis* strain CCUG 48459T was cultured overnight in sterile TSB medium in an anaerobic growth chamber containing Oxoid AnaeroGen (Thermo Fisher Scientific) sachets to create the anaerobic atmosphere. Subsequently, bacteria were diluted 1:100 by adding 2 µL of liquid culture into medium in a sterilized, clear polystyrene 96-well plate to a final assay volume of 200 µL. Subsequently, BzLPRDSar was added to the bacteria from a filter sterilized stock in MQ-H_2O to give 2, 8, 32, and 128 µg/mL final concentrations. Then, bacteria were incubated at 37 °C for 3, 6, 12, 36, or 48 h. Plates containing *L. kalixensis* were kept incubating under anaerobic conditions at 5% CO_2 and 6% O_2 at 37°C. Subsequently, their absorbance was measured at 600 nm using a Varioskan Lux microplate reader (Thermo Fisher Scientific) over the duration of the experiment. Final values were reported at the OD_{600} value after 48 h. All individual samples were carried out in triplicate.

Biofilm inhibition assays

For biofilm inhibition experiments, *S. aureus* strain CCUG 35,571, *E. faecalis* strain CCUG 34,289, *B. cereus* strain UW85, *S. agalactiae* strain CCUG 4208T, and *S. epidermidis* strain ATCC 35,984 were cultured overnight in sterile BHI broth, while *L. kalixensis* strain CCUG 48459T was cultured overnight in sterilized BHI broth under anaerobic conditions in a growth chamber containing Oxoid AnaeroGen sachets. Sterilized, clear polystyrene 96-well plates were prepared by coating with plasma by the addition of 20% of the final assay volume of Coagulase Test dissolved in 3 mL of sterilized distilled water to the wells and incubating overnight at 4°C. Then, the cultured strain was diluted 1:100 by adding 2 µL into BHI medium on the plasma-coated plate to a total volume of 200 µL. Subsequently, BzLPRDSar was added to the bacteria from filter-sterilized stocks in MQ-H_2O to give 8, 32, and 128 µg/mL final concentrations and incubated for 16 h at 37°C without shaking. The *L. kalixensis* strain was kept incubating under anaerobic conditions as described previously. Then, the supernatant was removed, and the wells were rinsed with PBS, 200 µL of 1% CV solution (diluted in PBS) was added, and the biofilms were stained for 10 min. The wells were washed with PBS twice, and 200 µL of a 95% ethanol solution in water was added to solubilize the cells for 30 min. A total of 100 µL of suspension was transferred into a new 96-well plate, and the absorbance was measured at 595 nm using a Varioskan Lux microplate reader (Thermo Fisher Scientific). All individual samples were carried out in triplicate.

SEM measurements

For SEM imaging, *S. aureus* strain CCUG 3557 and *S. epidermidis* strain ATCC 35,984 were cultured overnight in sterile TSB medium. Then, the cultured strain was diluted 1:100 into sterile TSB medium, and BzLPRDSar was added to a final concentration of

128 µg/mL. Cells grown in medium without any treatment were used as the control. After 16 h of incubation, the cells were washed and fixed in 3% glutaraldehyde for 2 h. Finally, the fixed samples were dehydrated with a series of washes with increasing ethanol concentration (40%, 50%, 60%, 70%, 80%, 90%, and 100%) for 10 min each and then dried for 2 h at room temperature. Before imaging, the dried samples were sputter coated with gold (5 nm). SEM imaging was performed with a Supra 60 VP (Carl Zeiss AG) microscope.

ACKNOWLEDGMENTS

The Knut and Alice Wallenberg Foundation via the Wallenberg Center for Molecular and Translational Medicine (A.A.T.), Swedish Research Council (2020-04299 and 2025-05306 to A.A.T.), Cancerfonden (22-2409 to A.A.T.), and Center for Antibiotic Resistance Research (CARe) are gratefully acknowledged. The authors thank Santosh Pandit for providing the multidrug-resistant *S. aureus*, *E. faecalis*, and *K. pneumoniae* bacterial strains and Mirjam Dannborg for help with setting up experiments under anaerobic growth conditions and providing the *L. kalixensis* strain.

AUTHOR AFFILIATIONS

[1]Department of Chemistry and Molecular Biology, University of Gothenburg, Gothenburg, Sweden
[2]Wallenberg Center for Molecular and Translational Medicine, University of Gothenburg, Göteborg, Sweden
[3]Division of Systems and Synthetic Biology, Department of Biology and Biological Engineering, Chalmers University of Technology, Göteborg, Sweden
[4]Center for Biosustainability, The Novo Nordisk Foundation, Technical University of Denmark, Kongens, Lyngby, Denmark

PRESENT ADDRESS

Jordi C. J. Hintzen, Department of Biochemistry and Biophysics, University of Pennsylvania, Perelman School of Medicine, Philadelphia, Pennsylvania, USA

AUTHOR ORCIDs

Jordi C. J. Hintzen http://orcid.org/0000-0002-4621-0711
Alesia A. Tietze http://orcid.org/0000-0002-9281-548X

FUNDING

Funder	Grant(s)	Author(s)
Knut och Alice Wallenbergs Stiftelse	WCMTM	Alesia A. Tietze
Swedish Research Council	2020-04299	Alesia A. Tietze
Cancerfonden	22-2409	Alesia A. Tietze

AUTHOR CONTRIBUTIONS

Jordi C. J. Hintzen, Conceptualization, Data curation, Formal analysis, Investigation, Methodology, Validation, Visualization, Writing – original draft, Writing – review and editing | Shadi Rahimi, Methodology, Supervision | Daniel Tietze, Data curation, Investigation, Methodology, Software, Visualization, Writing – original draft | Jian Zhang, Investigation, Methodology, Validation | Priyanka Mehra, Formal analysis, Visualization | Ivan Mijakovic, Resources | Alesia A. Tietze, Conceptualization, Data curation, Funding acquisition, Project administration, Resources, Software, Supervision, Writing – review and editing

ADDITIONAL FILES

The following material is available online.

Supplemental Material

Supplemental figures (Spectrum02327-25-s0001.docx). Fig. S1 to S5.

REFERENCES

1. Holmes NE, Howden BP. 2011. The rise of antimicrobial resistance: a clear and present danger. Expert Rev Anti Infect Ther 9:645–648. https://doi.org/10.1586/eri.11.49
2. Bai AD, Lo CKL, Komorowski AS, Suresh M, Guo K, Garg A, Tandon P, Senecal J, Del Corpo O, Stefanova I, Fogarty C, Butler-Laporte G, McDonald EG, Cheng MP, Morris AM, Loeb M, Lee TC. 2022. *Staphylococcus aureus* bacteraemia mortality: a systematic review and meta-analysis. Clin Microbiol Infect 28:1076–1084. https://doi.org/10.1016/j.cmi.2022.03.015
3. Leclercq R. 2009. Epidemiological and resistance issues in multidrug-resistant staphylococci and enterococci. Clin Microbiol Infect 15:224–231. https://doi.org/10.1111/j.1469-0691.2009.02739.x
4. Ribeiro da Cunha B, Fonseca LP, Calado CRC. 2019. Antibiotic discovery: where have we come from, where do we go? Antibiotics (Basel) 8:45. https://doi.org/10.3390/antibiotics8020045
5. Renwick M, Mossialos E. 2018. What are the economic barriers of antibiotic R&D and how can we overcome them? Expert Opin Drug Discov 13:889–892. https://doi.org/10.1080/17460441.2018.1515908
6. Dehbanipour R, Ghalavand Z. 2022. Anti-virulence therapeutic strategies against bacterial infections: recent advances. Germs 12:262–275. https://doi.org/10.18683/germs.2022.1328
7. Ruer S, Pinotsis N, Steadman D, Waksman G, Remaut H. 2015. Virulence-targeted antibacterials: concept, promise, and susceptibility to resistance mechanisms. Chem Biol Drug Des 86:379–399. https://doi.org/10.1111/cbdd.12517
8. Dickey SW, Cheung GYC, Otto M. 2017. Different drugs for bad bugs: antivirulence strategies in the age of antibiotic resistance. Nat Rev Drug Discov 16:457–471. https://doi.org/10.1038/nrd.2017.23
9. Suree N, Jung ME, Clubb RT. 2007. Recent advances towards new anti-infective agents that inhibit cell surface protein anchoring in *Staphylococcus aureus* and other gram-positive pathogens. Mini Rev Med Chem 7:991–1000. https://doi.org/10.2174/138955707782110097
10. Fleitas Martínez O, Cardoso MH, Ribeiro SM, Franco OL. 2019. Recent advances in anti-virulence therapeutic strategies with a focus on dismantling bacterial membrane microdomains, toxin neutralization, quorum-sensing interference and biofilm inhibition. Front Cell Infect Microbiol 9:74. https://doi.org/10.3389/fcimb.2019.00074
11. Spirig T, Weiner EM, Clubb RT. 2011. Sortase enzymes in Gram-positive bacteria. Mol Microbiol 82:1044–1059. https://doi.org/10.1111/j.1365-2958.2011.07887.x
12. Dramsi S, Trieu-Cuot P, Bierne H. 2005. Sorting sortases: a nomenclature proposal for the various sortases of Gram-positive bacteria. Res Microbiol 156:289–297. https://doi.org/10.1016/j.resmic.2004.10.011
13. Clancy KW, Melvin JA, McCafferty DG. 2010. Sortase transpeptidases: insights into mechanism, substrate specificity, and inhibition. Biopolymers 94:385–396. https://doi.org/10.1002/bip.21472
14. Vengadesan K, Narayana SVL. 2011. Structural biology of Gram-positive bacterial adhesins. Protein Sci 20:759–772. https://doi.org/10.1002/pro.613
15. Selvaraj C, Priya RB, Singh SK. 2018. Exploring the biology and structural architecture of sortase role on biofilm formation in gram positive pathogens. Curr Top Med Chem 18:2462–2480. https://doi.org/10.2174/1568026619666181130133916
16. Jonsson I-M, Mazmanian SK, Schneewind O, Bremell T, Tarkowski A. 2003. The role of *Staphylococcus aureus* sortase A and sortase B in murine arthritis. Microbes Infect 5:775–780. https://doi.org/10.1016/s1286-4579(03)00143-6
17. Jin T, Mohammad M, Pullerits R, Ali A. 2021. Bacteria and host interplay in *Staphylococcus aureus* septic arthritis and sepsis. Pathogens 10:158. https://doi.org/10.3390/pathogens10020158
18. Hall-Stoodley L, Costerton JW, Stoodley P. 2004. Bacterial biofilms: from the natural environment to infectious diseases. Nat Rev Microbiol 2:95–108. https://doi.org/10.1038/nrmicro821
19. Hintzen JCJ, Abujubara H, Tietze D, Tietze AA. 2024. The complete assessment of small molecule and peptidomimetic inhibitors of sortase a towards antivirulence treatment. Chemistry 30:e202401103. https://doi.org/10.1002/chem.202401103
20. Zrelovs N, Kurbatska V, Rudevica Z, Leonchiks A, Fridmanis D. 2021. Sorting out the superbugs: potential of sortase A inhibitors among other antimicrobial strategies to tackle the problem of antibiotic resistance. Antibiotics (Basel) 10:164. https://doi.org/10.3390/antibiotics10020164
21. Cascioferro S, Raffa D, Maggio B, Raimondi MV, Schillaci D, Daidone G. 2015. Sortase A inhibitors: recent advances and future perspectives. J Med Chem 58:9108–9123. https://doi.org/10.1021/acs.jmedchem.5b00779
22. Alharthi S, Alavi SE, Moyle PM, Ziora ZM. 2021. Sortase A (SrtA) inhibitors as an alternative treatment for superbug infections. Drug Discov Today 26:2164–2172. https://doi.org/10.1016/j.drudis.2021.03.019
23. Abujubara H, Hintzen JCJ, Rahimi S, Mijakovic I, Tietze D, Tietze AA. 2023. Substrate-derived sortase A inhibitors: targeting an essential virulence factor of Gram-positive pathogenic bacteria. Chem Sci 14:6975–6985. https://doi.org/10.1039/d3sc01209c
24. Ch'ng J-H, Chong KKL, Lam LN, Wong JJ, Kline KA. 2019. Biofilm-associated infection by enterococci. Nat Rev Microbiol 17:82–94. https://doi.org/10.1038/s41579-018-0107-z
25. Barnes AMT, Frank KL, Dale JL. 2021. *Enterococcus faecalis* colonizes and forms persistent biofilm microcolonies on undamaged endothelial surfaces in a rabbit endovascular infection model. FEMS Microbes 2:xtab018. https://doi.org/10.1093/femsmc/xtab018
26. Houry A, Briandet R, Aymerich S, Gohar M. 2010. Involvement of motility and flagella in *Bacillus cereus* biofilm formation. Microbiology (Reading, Engl) 156:1009–1018. https://doi.org/10.1099/mic.0.034827-0
27. Koehler TM. 2009. *Bacillus anthracis* physiology and genetics. Mol Aspects Med 30:386–396. https://doi.org/10.1016/j.mam.2009.07.004
28. Rossi F, Amadoro C, Colavita G. 2019. Members of the *Lactobacillus* genus complex (LGC) as opportunistic pathogens: a review. Microorganisms 7:126. https://doi.org/10.3390/microorganisms7050126
29. Rosini R, Margarit I. 2015. Biofilm formation by *Streptococcus agalactiae*: influence of environmental conditions and implicated virulence factors. Front Cell Infect Microbiol 5:6. https://doi.org/10.3389/fcimb.2015.00006
30. Gao J, Yu F-Q, Luo L-P, He J-Z, Hou R-G, Zhang H-Q, Li S-M, Su J-L, Han B. 2012. Antibiotic resistance of *Streptococcus agalactiae* from cows with mastitis. Vet J 194:423–424. https://doi.org/10.1016/j.tvjl.2012.04.020
31. O'Gara JP, Humphreys H. 2001. *Staphylococcus epidermidis* biofilms: importance and implications. J Med Microbiol 50:582–587. https://doi.org/10.1099/0022-1317-50-7-582
32. Selvaraj A, Valliammai A, Sivasankar C, Suba M, Sakthivel G, Pandian SK. 2020. Antibiofilm and antivirulence efficacy of myrtenol enhances the antibiotic susceptibility of *Acinetobacter baumannii*. Sci Rep 10:21975. https://doi.org/10.1038/s41598-020-79128-x
33. Waterhouse AM, Procter JB, Martin DMA, Clamp M, Barton GJ. 2009. Jalview Version 2—a multiple sequence alignment editor and analysis workbench. Bioinformatics 25:1189–1191. https://doi.org/10.1093/bioinformatics/btp033
34. Sievers F, Wilm A, Dineen D, Gibson TJ, Karplus K, Li W, Lopez R, McWilliam H, Remmert M, Söding J, Thompson JD, Higgins DG. 2011. Fast, scalable generation of high-quality protein multiple sequence alignments using Clustal Omega. Mol Syst Biol 7:539. https://doi.org/10.1038/msb.2011.75
35. Gao M, Johnson DA, Piper IM, Kodama HM, Svendsen JE, Tahti E, Longshore-Neate F, Vogel B, Antos JM, Amacher JF. 2022. Structural and biochemical analyses of selectivity determinants in chimeric

Streptococcus Class A sortase enzymes. Protein Sci 31:701–715. https://doi.org/10.1002/pro.4266
36. Johnson DA, Piper IM, Vogel BA, Jackson SN, Svendsen JE, Kodama HM, Lee DE, Lindblom KM, McCarty J, Antos JM, Amacher JF. 2022. Structures of *Streptococcus pyogenes* class A sortase in complex with substrate and product mimics provide key details of target recognition. J Biol Chem 298:102446. https://doi.org/10.1016/j.jbc.2022.102446
37. Bradshaw WJ, Davies AH, Chambers CJ, Roberts AK, Shone CC, Acharya KR. 2015. Molecular features of the sortase enzyme family. FEBS J 282:2097–2114. https://doi.org/10.1111/febs.13288
38. Kappel K, Wereszczynski J, Clubb RT, McCammon JA. 2012. The binding mechanism, multiple binding modes, and allosteric regulation of *Staphylococcus aureus* Sortase A probed by molecular dynamics simulations. Protein Sci 21:1858–1871. https://doi.org/10.1002/pro.2168
39. Piper IM, Struyvenberg SA, Valgardson JD, Johnson DA, Gao M, Johnston K, Svendsen JE, Kodama HM, Hvorecny KL, Antos JM, Amacher JF. 2021. Sequence variation in the β7-β8 loop of bacterial class A sortase enzymes alters substrate selectivity. J Biol Chem 297:100981. https://doi.org/10.1016/j.jbc.2021.100981
40. Krieger E, Vriend G. 2014. YASARA View - molecular graphics for all devices - from smartphones to workstations. Bioinformatics 30:2981–2982. https://doi.org/10.1093/bioinformatics/btu426
41. Krieger E, Vriend G. 2015. New ways to boost molecular dynamics simulations. J Comput Chem 36:996–1007. https://doi.org/10.1002/jcc.23899
42. Tang Z, Jiang W, Li S, Huang X, Yang Y, Chen X, Qiu J, Xiao C, Xie Y, Zhang X, Li J, Verma CS, He Y, Yang A. 2023. Design and evaluation of tadpole-like conformational antimicrobial peptides. Commun Biol 6:1177. https://doi.org/10.1038/s42003-023-05560-0
43. Priester JH, Horst AM, Van de Werfhorst LC, Saleta JL, Mertes LAK, Holden PA. 2007. Enhanced visualization of microbial biofilms by staining and environmental scanning electron microscopy. J Microbiol Methods 68:577–587. https://doi.org/10.1016/j.mimet.2006.10.018
44. Bozhkova SA, Gordina EM, Labutin DV, Netyl'ko GI, Ivantcova PM, Kudryavtsev KV. 2024. Evaluation of LPRDA pentapeptide for the prevention and treatment of *Staphylococcus aureus* peritoneal infection. Int J Mol Sci 25:11926. https://doi.org/10.3390/ijms252211926